LBL-22160

Lawrence Berkeley Laboratory

UNIVERSITY OF CALIFORNIA

Materials & Molecular Research Division

MAR 2 1987

Presented at the International Materials Symposium, Ceramic Microstructures '86: Role of Interfaces, Berkeley, CA, July 28-31, 1986

ORIGIN OF CRACKING PHENOMENA OBSERVED IN DECOMPOSITION REACTIONS

M.G. Kim, U. Dahmen and A.W. Searcy

November 1986

TWO-WEEK LOAN COPY

This is a Library Circulating Copy which may be borrowed for two weeks.

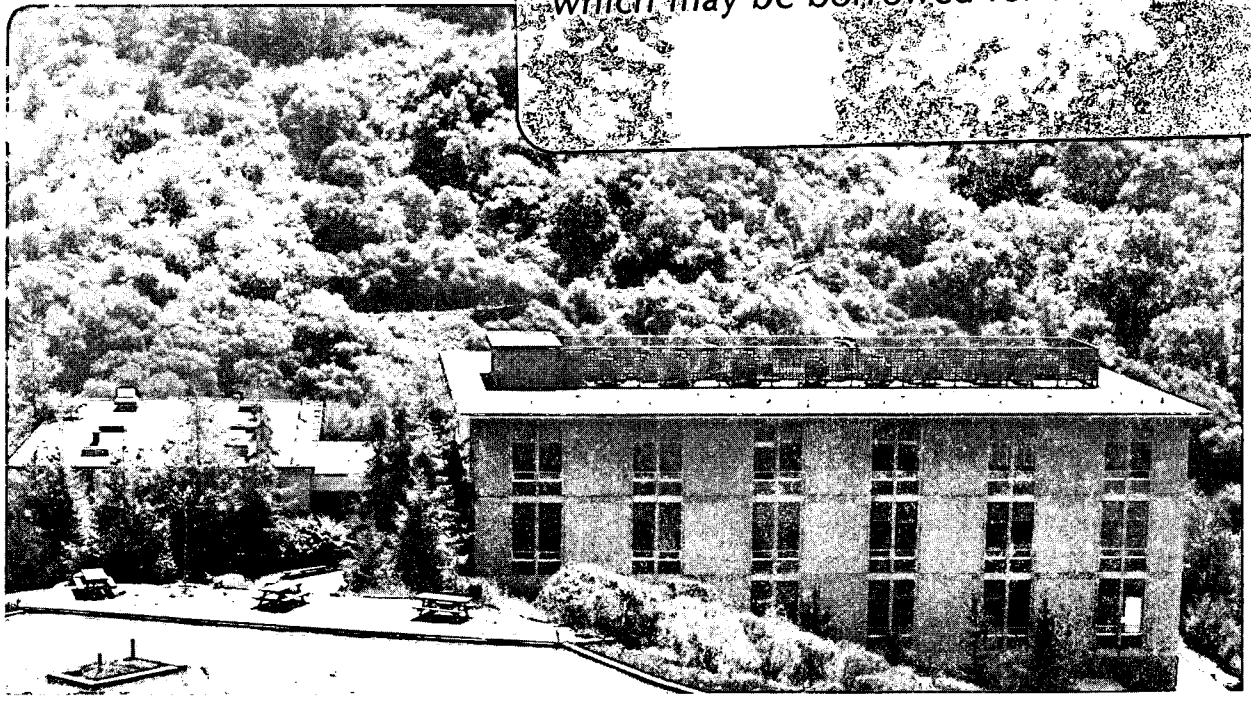

Prepared for the U.S. Department of Energy under Contract DE-AC03-76SF00098

LBL-22160

DISCLAIMER

This document was prepared as an account of work sponsored by the United States Government. While this document is believed to contain correct information, neither the United States Government nor any agency thereof, nor the Regents of the University of California, nor any of their employees, makes any warranty, express or implied, or assumes any legal responsibility for the accuracy, completeness, or usefulness of any information, apparatus, product, or process disclosed, or represents that its use would not infringe privately owned rights. Reference herein to any specific commercial product, process, or service by its trade name, trademark, manufacturer, or otherwise, does not necessarily constitute or imply its endorsement, recommendation, or favoring by the United States Government or any agency thereof, or the Regents of the University of California. The views and opinions of authors expressed herein do not necessarily state or reflect those of the United States Government or any agency thereof or the Regents of the University of California.

LBL-22160

ORIGIN OF CRACKING PHENOMENA OBSERVED IN DECOMPOSITION REACTIONS

M.G. Kim, U. Dahmen and Alan W. Searcy

Materials and Molecular Research Division
Lawrence Berkeley Laboratory and Department
of Materials Science and Mineral Engineering
University of California
Berkeley, California 94720

INTRODUCTION

Thermal decomposition, often referred to as calcination, is one of the important steps in ceramic processing. Decomposition reactions are of particular interest because they produce highly active solids of large surface areas[1-3]. But the high reactivity of fine powders is often limited by agglomeration and/or aggregation problems[2,4]. Furthermore large voids developed by cracking during the decomposition reaction can limit the densification of fine powders.

Extensive cracking was observed by Gordon and Kingery[5] and Freund[6] during decomposition of $Mg(OH)_2$. The cracks penetrated through the undecomposed $Mg(OH)_2$ in a network of 1-3 μm mesh size. In their decomposition study of $Mg(OH)_2$ by optical and transmission electron microscopy (TEM) Gordon and Kingery[5] concluded that the cracking occurred to relieve a critical strain arising from the coherent nucleation of MgO in the $Mg(OH)_2$ matrix. The basis for their conclusion was twofold, i) $Mg(OH)_2$ cracked before all the water was expelled and ii) an observed shift of MgO diffraction spots indicated a gradual decrease of the Mg-Mg distance from that in $Mg(OH)_2$ to that in normal MgO. Based on his X-ray and scanning electron microscopy (SEM) study, Freund[6] also attributed the cracking to strain at the reaction

interface resulting from the slight lattice contraction when $Mg(OH)_2$ dehydrated to an intermediate defect phase $Mg(OH)_{2-x}O_{x/2}\,\square_{x/2}$, with $x \longrightarrow 2$. He concluded that after this cracking, cubic MgO crystallized with a larger lattice contraction as 5-10 nm MgO crystallites.

Cracking was also observed by Beruto et al.[7] in the decomposition of $CaCO_3$. They reported a duplex pore structure, i.e., pores of ~5 nm and others of ~1 μm cross section and proposed that the larger pores (cracks) were due to a diffusionless repacking of CaO particles which had initially formed with a more uniform distribution of particles and pores.

Although the cracking in topotactic decomposition reactions appears to be a general phenomenon, it is still not well understood. In order to develop a better understanding of its origin the decomposition of $Mg(OH)_2$ and $MgCO_3$ was investigated by TEM and SEM. Since $Mg(OH)_2$ and $MgCO_3$ yield the same product solid from different parent structures a comparative study of their decomposition is expected to shed light on the structural origins of the cracking phenomena.

MATERIALS AND EXPERIMENTAL PROCEDURES

Materials

The materials used in this study are mineral $Mg(OH)_2$ (brucite)* and $MgCO_3$ (magnesite)**. Approximate formulas based on spectrographic analyses are as follows: brucite; $Mg_{0.995}Mn_{0.004}Fe_{0.0005}Ca_{0.00005}$

$(OH)_2$ and magnesite; $Mg_{0.979}Si_{0.01}Fe_{0.0005}Ca_{0.003}Mn_{0.0001}CO_3$. The X-ray powder diffraction measurements showed that the above two materials had the normal structures of $Mg(OH)_2$ and $MgCO_3$.

Transmission and Scanning Electron Microscopy

Thin foils of $Mg(OH)_2$ and $MgCO_3$ were prepared by the cleavage method and ion-beam milling, respectively[8]. All the TEM specimens were sandwiched between 150 mesh copper folding grids of which one inner side had been covered with a thin carbon film. This sandwich arrangement of specimens effectively prevented electron charging of the non-conducting materials.

The TEM specimens were examined in Hitachi 650, Kratos 1500, Siemens 102, and JEOL 200 CX microscopes. $Mg(OH)_2$ and $MgCO_3$ crystals were decomposed in-situ by either electron beam illumination or hot stage heating.

Precise lattice parameter measurements were made with specimens on which gold had been vapor deposited as a standard. Mixed diffraction patterns of gold and the specimen were recorded on glass plates and distances between diffraction spots were measured by means of a microdensitometer. The use of glass plates eliminated any bending or shrinkage when recorded negatives were under light illumination for a microdensitometer measurement. Lattice parameter calibrations with gold films and $Mg(OH)_2$ and $MgCO_3$ reactant solids showed that the accuracy of this measurement was better than $\pm$ 0.1%.

* Wood's mine, Texas, Pennsylvania
** Djebel Hadifa, Algeria

Specimens for SEM observation were prepared by thermal decomposition of $Mg(OH)_2$ and $MgCO_3$ crystals in a thermogravimetric apparatus in a vacuum of ~10^{-4} Torr (1.33×10^{-2} Pa). The specimens covered with a gold film of ~3 nm thickness were observed in an ISI-130 SEM with a maximum resolution of about 3 nm.

RESULTS AND DISCUSSION

Both $Mg(OH)_2$ and $MgCO_3$ decompose topotactically to yield porous pseudomorphic MgO of normal structure with definite orientation relationships. The decomposition of $Mg(OH)_2$ (a_o = 0.3147 nm, c_o = 0.4769 nm; space group P3m) yields MgO (a_o = 0.4213 nm; space group $Fm\bar{3}m$) with a single orientation relationship; (0001) $Mg(OH)_2$ //(111) MgO, $[11\bar{2}0]$ $Mg(OH)_2$// $[10\bar{1}]$ MgO.[5,8,9] But that of $MgCO_3$ (a_o = 0.46332 nm, c_o = 1.5015 nm; space group $R\bar{3}c$) has two variants of a major orientation relationship; (0001) $MgCO_3$ //(111) MgO, $[11\bar{2}0]$ $MgCO_3$//$[2\bar{1}\bar{1}]$ MgO.[8] The porosities of MgO resulting from the pseudomorphic decomposition of $Mg(OH)_2$ and $MgCO_3$ are about 54% and 60%, respectively.

Figure 1A shows ~2 nm cubic MgO particles formed from the decomposition of $Mg(OH)_2$ at ~600 k. Cubic MgO particles of ~3 nm edge length, formed from the decomposition of $MgCO_3$ at ~800 K, are shown in Fig. 1B. The inserted diffraction pattern illustrates the two orientation variants of the MgO particles, rotated 60 degrees relative to each other around their common three-fold axis.[8]

Partially decomposed specimens of $Mg(OH)_2$ and $MgCO_3$ exhibited cracks as shown in Fig. 2. The inserted electron diffraction patterns taken just after cracking clearly show the diffraction spots of

reactant and product solids. As mentioned above, previous investigators proposed that the cracking occurred to relieve the elastic strains arising from coherent nucleation of MgO in the $Mg(OH)_2$ matrix. However, MgO diffraction spots of normal lattice parameter were observed before any cracking occurred. (A possible explanation of the abnormal parameter measured by Gordon and Kingery[5] has been suggested.[8] Also local decomposition by electron beam illumination produced the MgO particles without any cracking (Fig. 3). The MgO particles are ~2 nm cubes (Fig. 1A), precluding any appreciable elastic strain at the reaction interface. These findings are inconsistent with the hypothesis of previous investigators for the cracking in the decomposition of $Mg(OH)_2$.

While the orientation relationship of $Mg(OH)_2$ decomposition predicts a plausible coherent plane, that of $MgCO_3$ decomposition excludes any possible coherent plane.[8] This fact also suggests that the cracking is not a consequence of an elastic strain but of some other driving force. The only identifiable driving force for the cracking is the high excess surface energy arising from the small MgO particles. In order to reduce the free energy the small particles would aggregate. The aggregation of such small particles could develop the cracks.

The different crack morphologies resulting from the decomposition of $Mg(OH)_2$ and $MgCO_3$ are shown in Fig. 4. The decomposition of $Mg(OH)_2$ formed a continuous network of cracks of about 2 μm mesh size while the decomposition of $MgCO_3$ produced cracks which radiated from isolated

centers. This difference might be due to the fact that the reactant solids have different densities of defects, i.e., of heterogeneous nucleation sites for the decomposition. $MgCO_3$ had a clean single crystalline form in TEM observation while $Mg(OH)_2$ showed a mottled structure due to a high density of inherent defects[9,10] (see Fig. 3). Thus the decomposition of $MgCO_3$ would be a nucleation-limited reaction with clearly bounded decomposed areas (Fig. 2B) while decomposition of $Mg(OH)_2$ would be a growth-limited reaction with a more homogeneous appearance.

These different crack morphologies were also observed by SEM with MgO produced from the decomposition of large crystals of $Mg(OH)_2$ and $MgCO_3$ (Figs. 5 & 6). $Mg(OH)_2$ decomposition (Fig. 5B) did not show a clear reaction interface while $MgCO_3$ decomposition (Fig. 6B) showed the reaction interface clearly. Figure 5 shows the crack patterns formed from the decomposition of $Mg(OH)_2$. Figure 5C may result from cracking along weakly bonded (0001) $Mg(OH)_2$ planes due to shear forces. When aggregation of the oriented MgO particles occurs, $Mg(OH)_2$ at the reaction interface would experience a stress which could nucleate and propagate the observed cracks along the [0001] direction. Simultaneously a shear force may cause cracking along the weakly bonded [0001] layers.

One interesting feature of the cracks is the observation that they penetrate into the $Mg(OH)_2$ but not into the $MgCO_3$. This difference may be due to the different strength of the reactant solids, or may more likely be a result of the fact that MgO cubes of a

single orientation variant aggregate more easily than the homogeneous mixture of two orientation variants observed to form during $MgCO_3$ decomposition.

Another interesting feature of the $Mg(OH)_2$ decomposition at 900 K was the development of radial crack patterns around isolated holes as shown in Fig. 7. These are likely to have developed from the eruption of product gas. The exothermic aggregation of MgO particles may be triggered by the eruption of gas trapped near the reaction interface or vice versa, the heat released by local aggregation may cause accelerated decomposition leading to a local increase in gas pressure. This hypothesis is further supported by the TEM observation that the cracks did not form in very thin $Mg(OH)_2$ crystals.[11] Therefore the cracks may have a role in providing the routes for the easy escape for the product gases.

CONCLUSION

The development of cracks in the decomposition of $Mg(OH)_2$ and $MgCO_3$ was observed directly by TEM and SEM.

The only identifiable driving force for the cracking is the high excess surface energy of the product solid MgO particles of 2-3 nm cube edge. The cracks may form as a consequence of aggregation of these small particles to reduce the excess energy.

The decomposition of $Mg(OH)_2$ formed a continuous network of cracks of about 2 μm mesh size while the decomposition of $MgCO_3$ showed the cracks to radiate from isolated centers. This different crack morphology might result from the different orientation variants and the different defect densities of reactant solids.

ACKNOWLEDGEMENT

This work was supported by the Director, Office of Energy Research, Office of Basic Energy Sciences, Materials Sciences Division of the U.S. Department of Energy under contract Number DE-AC03-76SF00098.

REFERENCES

1. J.L. Pentecost, Powder Preparation Processes, in "Ceramic Fabrication Processes", F.F.Y. Wang, ed., Academic Press, New York (1976).

2. I.B. Cutler, Active Powders, in "Ceramic Processing Before Firing", G.Y. Onoda, Jr. and L.L. Hench, eds., John Wiley & Sons, New York (1978).

3. L. Volpe and M. Boudart, Topotactic Preparation of Powders with High Specific Surface Area, Catal. Rev.-Sci. Eng., 27: 515 (1985).

4. W.H. Rhodes, Agglomerate and Particle Size Effects on Sintering Yttria-Stablized Zirconia, J. Am. Ceram. Soc., 64: 19 (1981).

5. R.S. Gordon and W.D. Kingery, Thermal Decomposition of Brucite: I, Electron and Optical Microscope Studies, J. Am. Ceram. Soc., 49: 654 (1966).

6. F. Freund, Correlation Between Strain and Grain Sizes for the Thermal Decomposition of $Mg(OH)_2$ Single Crystals, Bev. Dtsch. Ker. Ges., 52: 53 (1975).

7. D. Beruto, L. Barco and A.W. Searcy, Rearrangement of Porous CaO Aggregates During Calcite Decomposition in Vacuum, J. Am. Ceram. Soc., 66: 893 (1983).

8. M.G. Kim, U. Dahmen and A.W. Searcy, Structural Transformations in the Decomposition of $Mg(OH)_2$ and $MgCO_3$, submitted for publication to J. Am. Ceram. Soc.

9. J.F. Goodman, Decomposition of Magnesium Hydroxide in an Electron Microscope, Proc. Roy. Soc. (London), A247: 346 (1958).

10. M.G. Kim, Kinetic and TEM Studies of Decomposition of $Mg(OH)_2$ and $MgCO_3$, Ph.D. Thesis, University of California, Berkeley, CA (1985).

11. M.G. Kim and U. Dahmen, Unpublished work.

FIGURES

1. TEM micrographs of MgO produced from the decomposition of $Mg(OH)_2$ (A) and $MgCO_3$ (B) showing aggregates of small MgO cubes in a [100] orientation in (A) and in both [100] and near-[110] orientations in (B), as expected from the orientation variants[8].

2. TEM micrographs of partly decomposed [0001] $Mg(OH)_2$ to [111] MgO (A) and $[10\bar{1}1]$ $MgCO_3$ to MgO (B). MgO diffraction spots in Fig. (B) are mirror-related across the $(1\bar{2}10)$ plane of $MgCO_3$.

3. TEM micrographs of $Mg(OH)_2$ which was locally decomposed by the electron beam; the bright center area of the picture is decomposed.

4. TEM micrographs of MgO produced from the decompositions of $Mg(OH)_2$ (A) and $MgCO_3$ (B).

5. SEM micrographs of partly decomposed $Mg(OH)_2$; (A) initial cleavage surface, (B) cleavage surface of middle of the crystal showing the cracked (top) and uncracked areas (bottom), and (C) edge surface normal to the cleavage surface.

6. SEM micrographs of partly decomposed $MgCO_3$; (A) initial cleavage surface and (B) cleavage surface of middle of the crystal showing the decomposed and undecomposed areas with the reaction interface.

7. SEM micrographs of MgO produced from $Mg(OH)_2$ decomposition; (A) initial cleavage surface decomposed at ~600K and (B) cleavage surface of middle of the crystal decomposed at ~900 K.

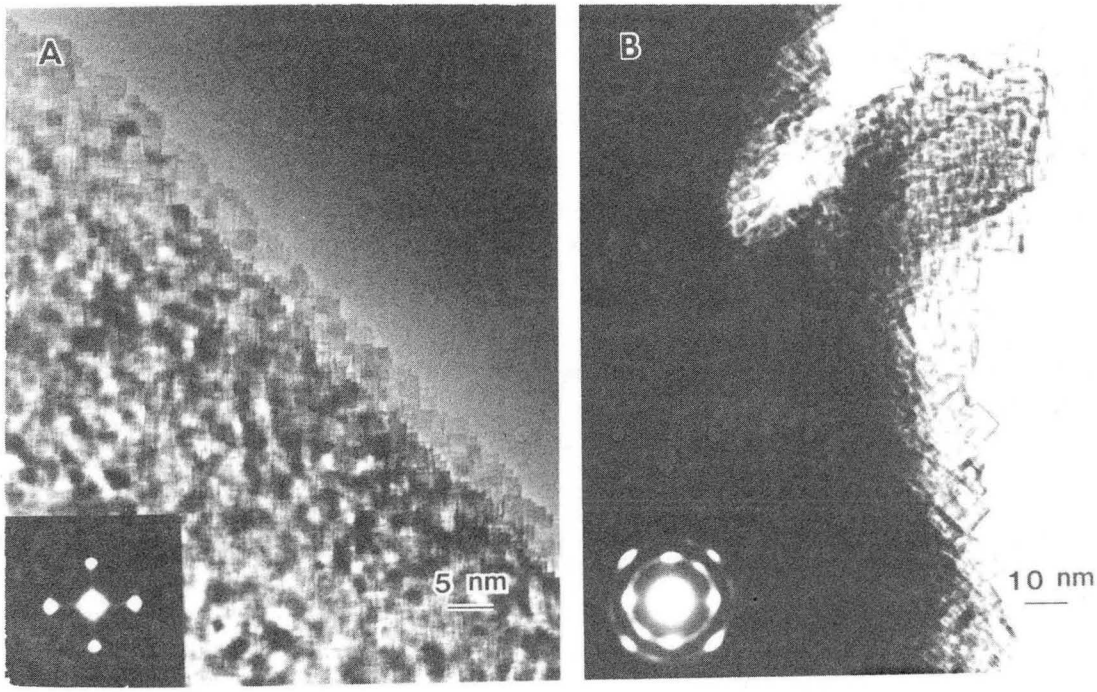

Fig. 1. TEM micrographs of MgO produced from the decomposition of $Mg(OH)_2$ (A) and $MgCO_3$ (B) showing aggregates of small MgO cubes in a [100] orientation in (A) and in both [100] and near-[110] orientations in (B) as expected from the orientation variants[8].

XBB 867-5723

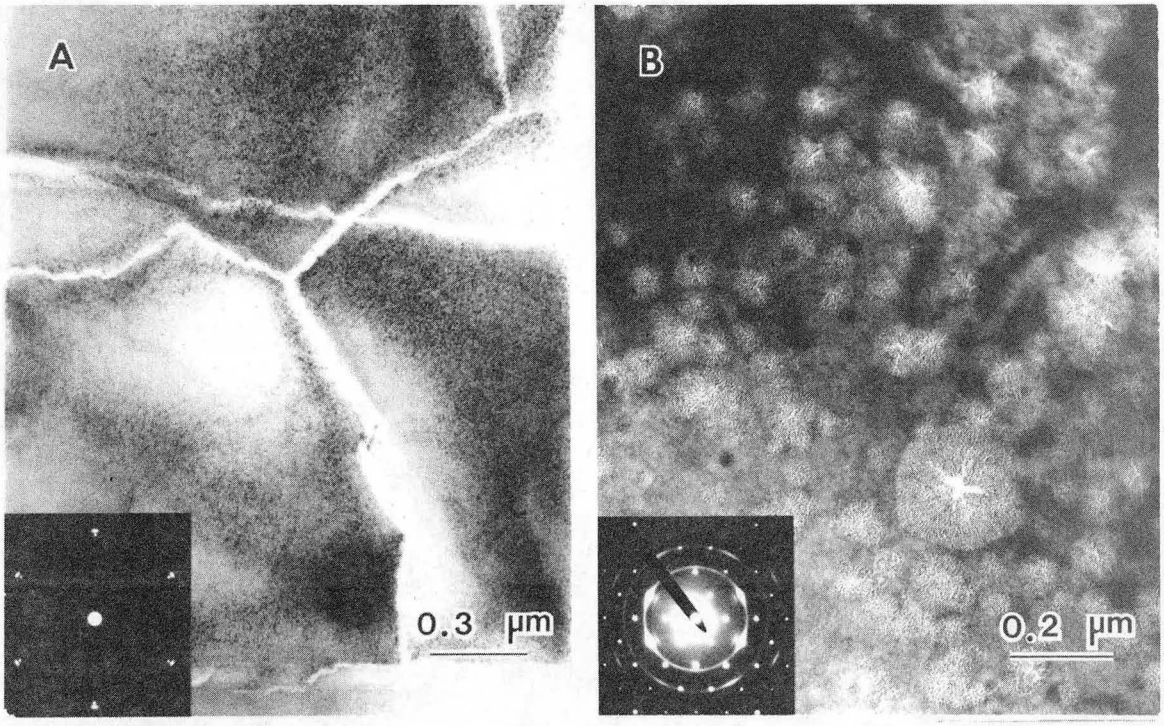

Fig. 2. TEM micrographs of partly decomposed [0001] $Mg(OH)_2$ to [111] MgO (A) and [$10\bar{1}1$] $MgCO_3$ to MgO (B). MgO diffraction spots in Fig. (B) are mirror-related across the ($1\bar{2}10$) plane of $MgCO_3$.

XBB 867-5724

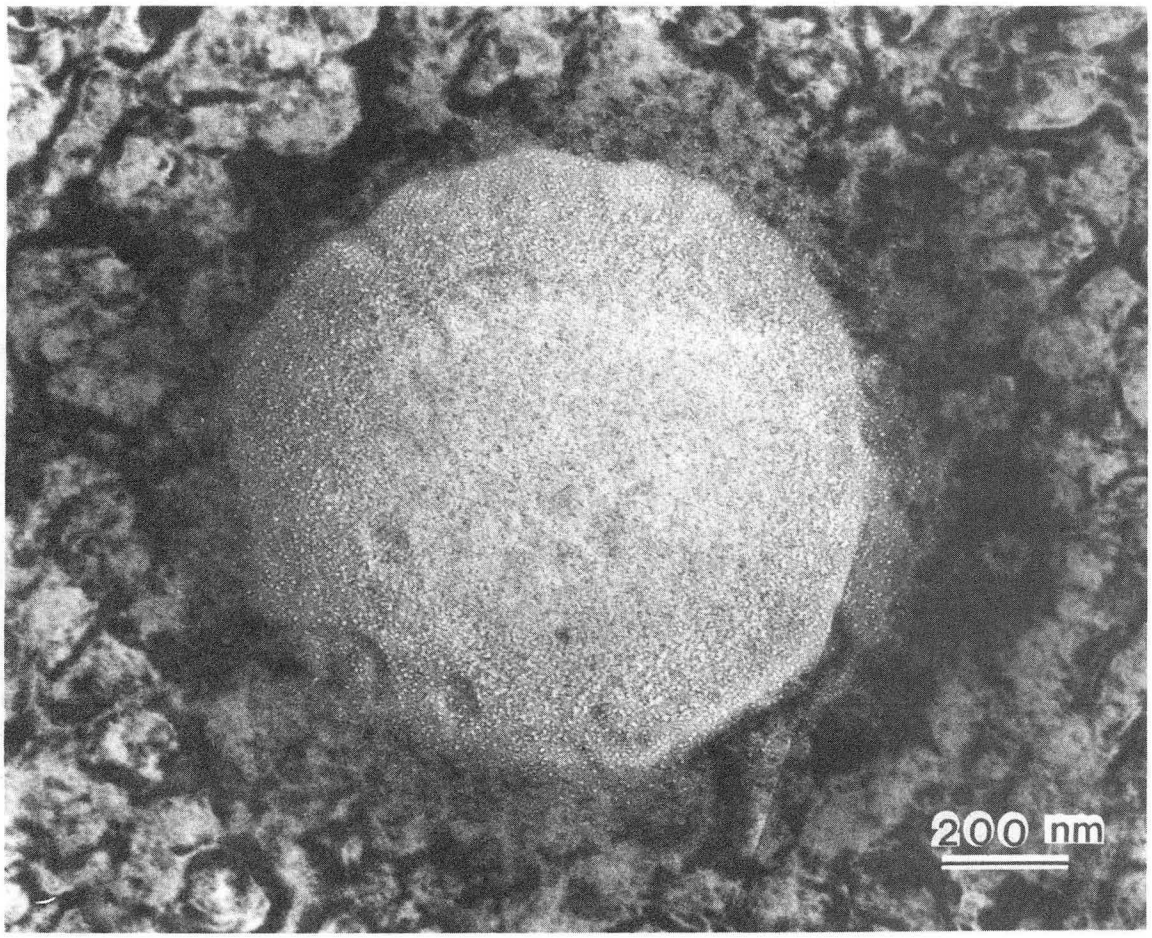

Fig. 3. TEM micrographs of $Mg(OH)_2$ which was locally decomposed by the electron beam; the bright center area of the picture is decomposed.

XBB 859-7042

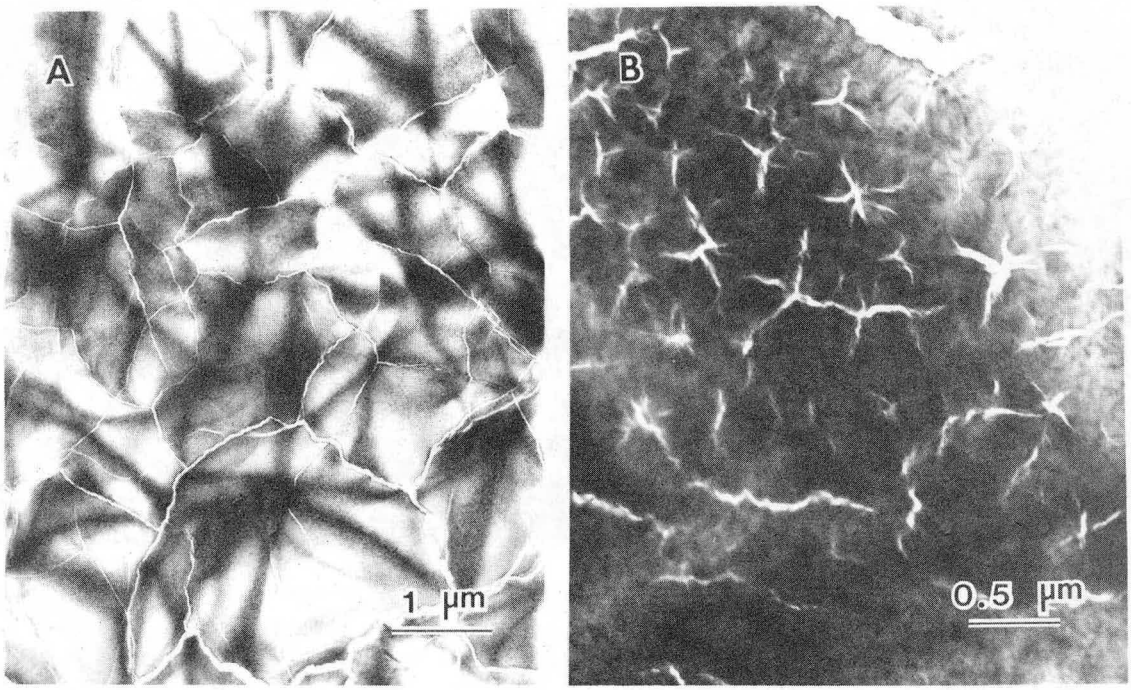

Fig. 4. TEM Micrographs of MgO produced from the decompositions of $Mg(OH)_2$ (A) and $MgCO_3$ (B).

XBB 867-5725

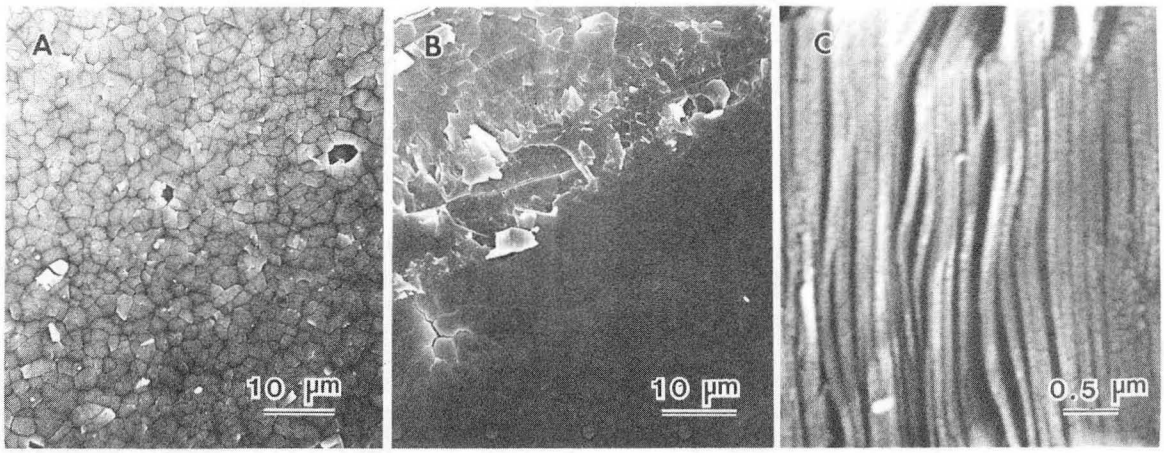

Fig. 5. SEM micrographs of partly decomposed $Mg(OH)_2$; (A) initial cleavage surface, (B) cleavage surface of middle of the crystal showing the cracked (top) and uncracked areas (bottom), and (C) edge surface normal to the cleavage surface.

XBB 867-5726

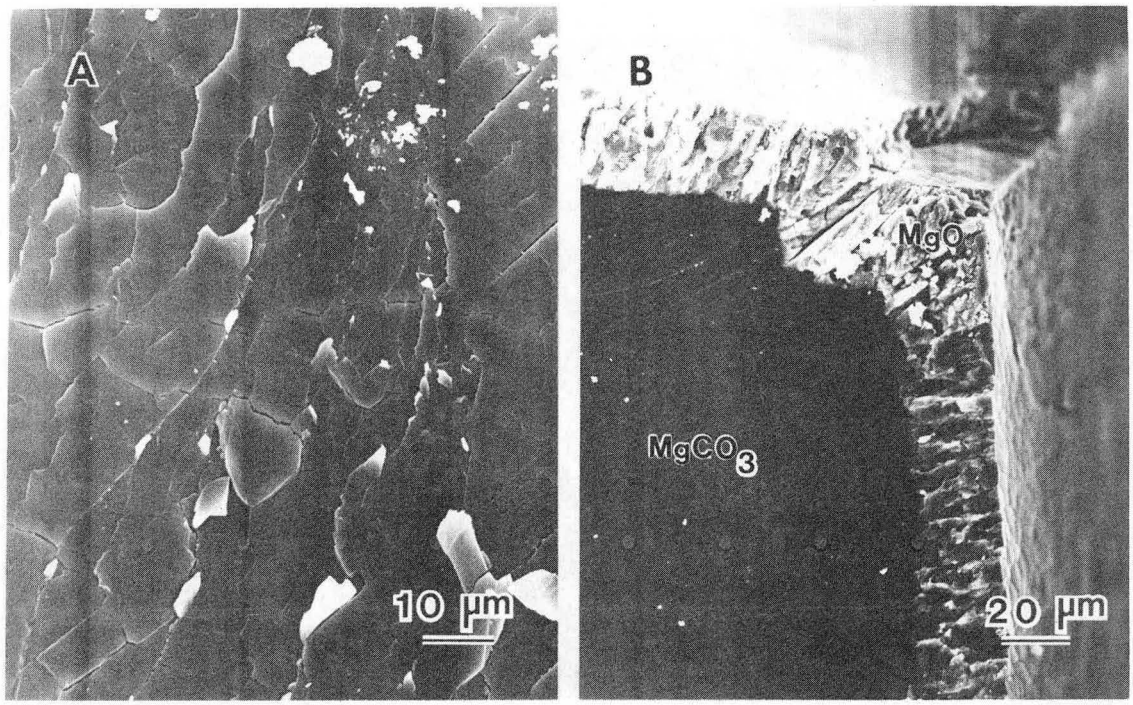

Fig. 6. SEM micrographs of partly decomposed $MgCO_3$; (A) initial cleavage surface and (B) cleavage surface of middle of the crystal showing the decomposed and undecomposed areas with the reaction interface.

XBB 867-5727

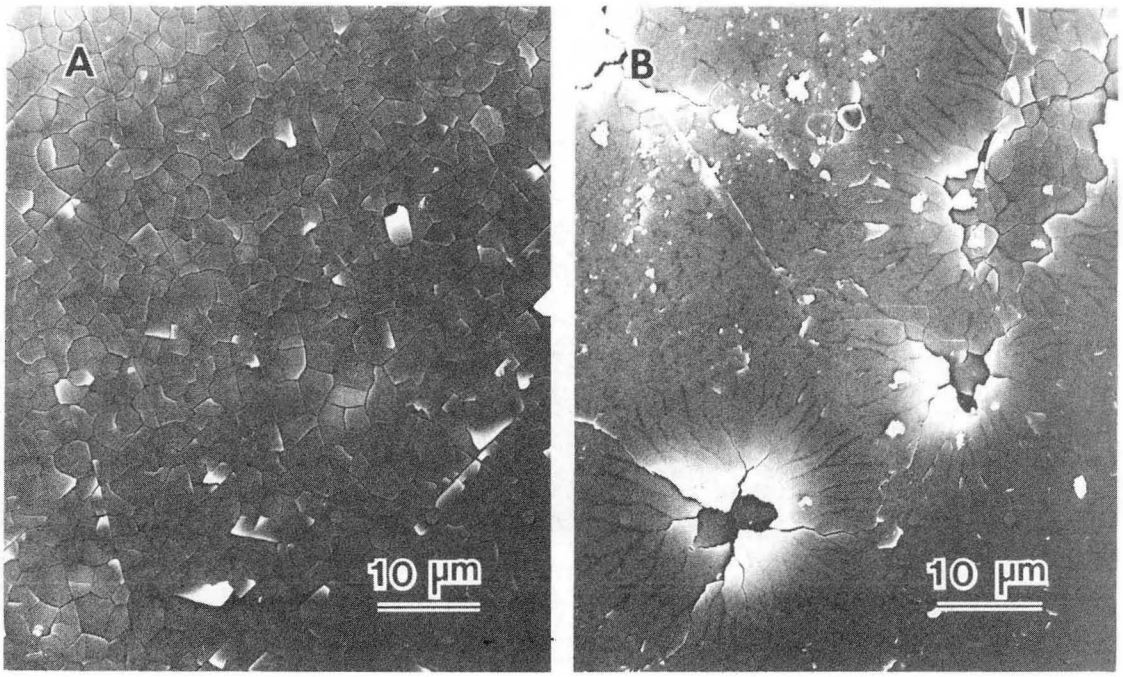

Fig. 7. SEM micrographs of MgO produced from $Mg(OH)_2$ decomposition; (A) initial cleavage surface decomposed at ∿600 K and (B) cleavage surface of middle of the crystal decomposed at ∿900 K.

XBB 867-5728

This report was done with support from the Department of Energy. Any conclusions or opinions expressed in this report represent solely those of the author(s) and not necessarily those of The Regents of the University of California, the Lawrence Berkeley Laboratory or the Department of Energy.

Reference to a company or product name does not imply approval or recommendation of the product by the University of California or the U.S. Department of Energy to the exclusion of others that may be suitable.

LAWRENCE BERKELEY LABORATORY
TECHNICAL INFORMATION DEPARTMENT
UNIVERSITY OF CALIFORNIA
BERKELEY, CALIFORNIA 94720